Effect of microphysical characteristics of suspensions on the backscattering characteristics of seawaters

V.V. Veretennikov

Institute of Atmospheric Optics,
Siberian Branch of the Russian Academy of Sciences, Tomsk

Received July 8, 2004

Effect of the disperse composition and the index of refraction of particles suspended in seawater on the scattering phase functions has been studied numerically within the scattering angles from 175 to 180°. We studied the effect produced by suspensions formed from mineral and organic particles at various proportions. A comparative analysis of the role of each fraction in the formation of the scattering phase functions was carried out. The possibilities of using the results of model calculations as an *a priori* information in interpretation of the data of laser sensing of seawaters are discussed.

Introduction

The efficiency of the solution of inverse problems of laser sensing of seawater depends, largely, on the correct use of *a priori* information on the medium under study. Scattering characteristics of seawater are determined by two main fractions of suspended particles having different microphysical characteristics.[1] The first fraction was formed by fine particles (with dimensions, which do not exceed 1–2 μm) of mineral (terrigenic) origin (t-fraction). The second fraction consists of larger particles of organic (biogenic) origin (b-fraction). The ratio of contributions to the total scattering coefficient of both fractions varies over a wide range. For example, according to data from Ref. 1 and depending on the type of water the contribution of particles of b-fraction to the scattering coefficient is from 22 to 78% that must naturally be represented by the form of the scattering phase function of such seawaters.

Previously[2] the investigations have been carried out of the effect of such a suspension on the scattering phase function in the range of small scattering angles. As shown in Ref. 2, in the formation of anisotropic part of the scattering phase function along with large particles of b-fraction small particles of t-fraction play a decisive role. For small-angle scattering phase function, the presence of two regions is typical, where the contributions from separate fractions dominate. The conventional boundary between these regions passes in the region of scattering angles of 1–2°. The scattering within the limits of the first, sufficiently narrow region is due to the particles of b-fraction, and the wider second region is mainly formed due to the scattering on particles of t-fraction.

The optical radiation propagation in the seawater is accompanied by the multiple light scattering. In this case the equations, used for describing the lidar returns should account for the multiple small-angle scattering and the single large-angle scattering.[3–5] Even at such a simplified description due to the multiple scattering the value of lidar return depends not only on the value of the scattering phase function in the direction of 180°, but also on its behavior in a certain vicinity of this direction.

As applied to the solution of problems of laser sensing of seawater of great importance are the data on the relation between the contributions coming from two fractions to the total backscattering phase function, which can be obtained using numerical modeling. The paper describes a numerical investigation of the effect of disperse composition and the refractive index of both fractions of particles suspended in seawater on the scattering phase function in the range of scattering angles of 175 to 180°. The possibilities are discussed of using the results of model calculations as *a priori* information when interpreting data of laser sensing of seawaters.

1. Two-component optical-microphysical model of suspension

As in the case of discussed in Ref. 2, in modeling the scattering phase functions of seawater it was considered that the suspension was formed by nonabsorbing particles. For describing the disperse composition of t-fraction in the paper, we used the size distribution function of particle geometrical cross sections of the power-law form

$$s_t(r) = \begin{cases} A_{t0}, & 0.01 \le r \le 0.05 \ \ \mu\text{m}, \\ A_t r^{-\nu}, & 0.05 \le r \le 2 \ \ \mu\text{m} \end{cases} \qquad (1)$$

with the index $\nu = 1–4$. The constant A_{t0} was chosen to meet the requirement of the function $s_t(r)$ continuity at the point $r = 0.05$ μm. According to the estimates[1] the relative refractive index of particles of t-fraction is $n_t = 1.15$. The particle-size distribution function of b-fraction was simulated using a modified gamma-distribution

0235-6880 / 04 / 09 681-05 $02.00

$$s_b(r) = A_b\left(\frac{r}{r_m}\right)^{\alpha}\exp\left\{-\frac{\alpha}{\gamma}\left[\left(\frac{r}{r_m}\right)^{\gamma}-1\right]\right\} \qquad (2)$$

with a varying modal radius r_m = 5–15 μm and the parameters $\alpha = 8$ and $\gamma = 3$. For the relative refractive index n_b the values were considered in the range 1.03–1.05. The weighting factors A_t and A_b in the distributions $s_t(r)$ and $s_b(r)$ were chosen so that to obtain a given ratio $\xi_p = \sigma_t / \sigma_b$ between the contributions of the above fractions to the total scattering coefficient $\sigma = \sigma_t + \sigma_b$.

For a considered model of the disperse suspension in water the calculations of the scattering phase functions were made

$$x(\theta) = p x_t(\theta) + (1-p) x_b(\theta). \qquad (3)$$

In Eq. (3) $x_t(\theta)$ and $x_b(\theta)$ are the scattering phase functions of t- and b-fractions of the suspension, respectively; the parameter $p = \sigma_t / \sigma$ determines the relative contribution of t-fraction to the total scattering coefficient. The condition of normalization for the above-mentioned scattering phase functions is as follows $\int_{4\pi} x(\theta)\,d\omega = 1$.

The paper presents some results of numerical investigations of the variability of scattering phase functions at the wavelength $\lambda = 0.532$ μm depending on microstructure parameters r_m, ν, and the ratio p. For the sake of convenience in analyzing below the obtained results, we use the following characteristics:

$$\xi_p = \sigma_t / \sigma_b = p/(1-p), \quad \xi_{\tilde{o}}(\theta) = x_t(\theta) / x_b(\theta), \qquad (4)$$

$$\xi(\theta) = p x_t(\theta) / [(1-p) x_b(\theta)] = \xi_p \xi_{\tilde{o}}(\theta), \qquad (5)$$

$$\omega(\theta) = p x_t(\theta) / x(\theta) = \xi / (\xi + 1), \qquad (6)$$

where ξ_p is the ratio between the scattering coefficients of the t- and b-fractions; $\xi_x(\theta)$ is the relation between the scattering phase functions for t- and b-fractions; $\xi(\theta)$ is the ratio between the t- and b-components of the total scattering phase function $x(\theta)$, Eq. (3); $\omega(\theta)$ is the relative contribution of the t-fraction to the total scattering phase function.

2. Analysis of scattering phase functions based on the results of numerical simulation

The results obtained by numerical simulation are depicted in Figs. 1 to 5. As an example Fig. 1*a* shows the scattering phase functions for separate fractions $x_t(\theta)$ and $x_b(\theta)$ as well as their weighted sum $x(\theta)$, Eq. (3), at $p = 0.2$ and the following values of microstructure parameters: r_m = 10 μm and $\nu = 2$. This example corresponds to the situation when b-fraction dominates ($\xi_p = 0.25$) in the total scattering. From Fig. 1*a* it follows that at scattering strictly backwards ($\theta = \pi$) the inequality $x_t(\pi) > x_b(\pi)$ works, and the relation between the scattering phase functions $\xi_x(\pi) = 2.27$. It should be noted that the scattering phase function of t-fraction, $x_t(\theta)$ weakly varies in the considered range of scattering angles $175 \le \theta \le 180°$ while the behavior of the scattering phase function of b-fraction, $x_b(\theta)$ is of more complicated nature and needs for further detailed consideration.

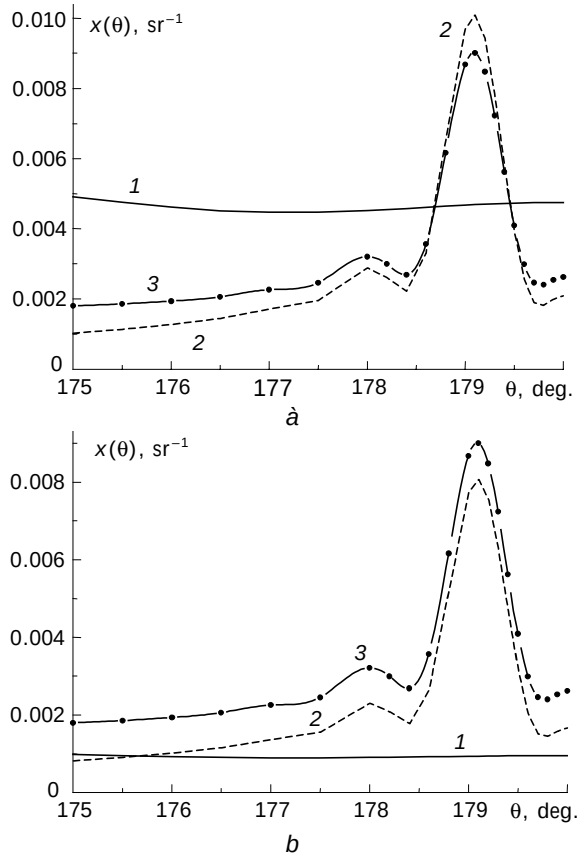

Fig. 1. Scattering phase functions $x_t(\theta)$ at $\nu = 2$ (curve *1*), $x_b(\theta)$ for the modal radius r_m = 10 μm (curve *2*) and their weighted sum $x(\theta)$ at $p = 0.2$ (curve *3*) (*à*); scattering phase function $x(\theta)$ (*3*) and its components $p x_t(\theta)$ (*1*), and $(1-p) x_b(\theta)$ (*2*), taken with the corresponding weights at the same microphysical parameters (*b*).

The main peculiarity of the function $x_b(\theta)$ is the pronounced maximum in the vicinity of the angle $\theta_1 = 179.1°$. The value of the scattering phase function $x_b(\theta_1)$ at the point of maximum exceeds its value in a backward direction by a factor of 4.8. One more, a less pronounced maximum of the function $x_b(\theta)$ is observed at $\theta_2 = 178°$. The position of the above-mentioned maxima of the scattering phase function $x_b(\theta)$ agrees well with the light diffraction theory in a backward direction.[6,7] According to Ref. 7 the angular distribution of light scattered by a large particle ($\rho \gg 1$, where ρ is the diffraction parameter of a particle) at small angles $\gamma = \pi - \theta$, $\gamma \sim 1/\rho$, $\gamma \ll 1$, is proportional to the linear combination of squares

of the Bessel functions of the zeroth-order and second order $J_i^2(z)$, $i = 0; 2$:

$$x(\theta) \sim c_0 J_0^2(\rho\gamma) + c_2 J_2^2(\rho\gamma) \qquad (7)$$

with the coefficients c_i depending on the size and the refractive index of particles. The result, similar to that presented by formula (7) without the first component, was obtained in Ref. 6. The first maxima of the functions $J_0^2(z)$ and $J_2^2(z)$ are positioned at the points $z_{0k} = 0$; 3.83... and $z_{2k} = 3.1$; 6.8..., respectively. One can associate the value of a certain effective particle radius with the position of such maxima of the scattering phase function by the formula

$$r_{\text{eff}} = z_i / k\gamma_i. \qquad (8)$$

For the function $x_b(\theta)$ shown in Fig. 1*a*, the estimation of the effective radius r_{eff} by formula (8) for values z_{2k}, corresponding to maxima of the function $J_2^2(z)$, gives the value within the limits from 12.4 to 12.6, close to the modal radius of b-fraction particles $r_m = 10$ μm.

Graphically the role of two fractions in the formation of the scattering phase function $x(\theta)$ is presented in Fig. 1*b* by its components $px_t(\theta)$ and $(1 - p)\, x_b(\theta)$ taken with the appropriate weights. The total scattering phase function $x(\theta)$ is here the same as in Fig. 1*a*. The relative contribution of t-fraction in the backscattering phase function $\omega(\pi) = 0.36$ and it is found to be almost twice as large as its contribution to the scattering coefficient $p = 0.2$. The relation between two components in the backscattering phase function $\xi(\pi) = 0.57$, while $\xi_p = 0.25$. One can easily follow the variation of the above-mentioned relations for the other scattering angles. From Eqs. (4) and (5), in particular, it follows that for scattering phase functions, shown in Fig. 1 the inequality $\xi(\theta) > \xi_p$ takes place almost everywhere, except for the proximity of the diffraction peak at $\theta = \theta_1$, within which $x_b(\theta) > x_t(\theta)$.

Figure 2 shows the parametric series of curves $x(\theta)$, Eq. (3), calculated as functions of the relation p using data presented in Fig. 1. Curve *1* corresponds to the case of $p = 0$ and describes the behavior of the scattering phase function for particles of the b-fraction $x(\theta) = x_b(\theta)$. In the general case the scattering phase function $x(\theta) = x(\theta, p)$, as a function of the parameter p, varies according to a linear law:

$$x(\theta) / x_b(\theta) = p(1 - \xi_x) + 1, \qquad (9)$$

where the value ξ_x is determined from Eq. (4), at $\xi_x > 1$, i.e., in those regions where $x_t(\theta) > x_b(\theta)$ (see Fig. 1*a*), the formula (9) determines, evidently, the linearly increasing function p with the range of variation $[1, \xi_x]$. On the contrary, at $\xi_x < 1$ the scattering phase function $x(\theta, p)$, as a function of p, linearly decreases. In this case the range of variation of Eq. (9) is $[\xi_x, 1]$. Curves in Fig. 2 have two common points of intersection corresponding to the case $\xi_x = 1$.

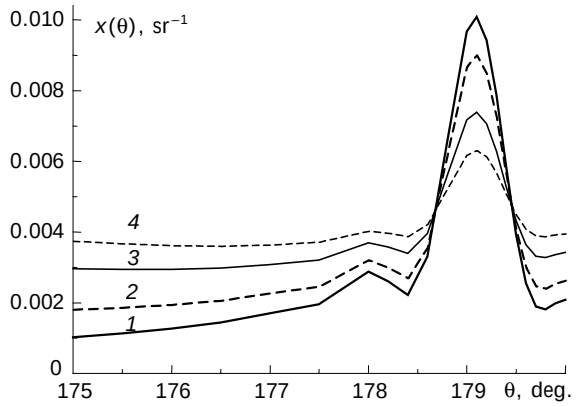

Fig. 2. Variability of the scattering phase function $x(\theta)$ depending on the contribution of t-fraction: $p = 0$ (*1*); 0.2 (*2*); 0.5 (*3*) and 0.7 (*4*) at $\nu = 2$, $r_m = 10$ μm.

The given relations are of a basic importance for solving inverse problems on the reconstruction of optical characteristics of suspensions using methods of laser sensing. If under observation conditions only the concentration of one of the fractions varies, then in the presence of the second fraction the backscattering phase function $x(\pi)$ does not remain constant. Its variation is determined by Eq. (9) that can be taken into account in the development of algorithms for the inversion of lidar returns.

In particular, in a considered example the backscattering phase function $x(\pi)$ can vary by 2.27 times at all kinds of variations of the relation between the suspension components. The constancy of the scattering phase function at lidar measurements can be provided at the cost of small (about 0.5°) shift from the strictly backward direction ($\theta = 180°$) to a direction defined by the position of the nearest point of intersection of the curves in Fig. 2, in which, as was already noted, $\xi_x = 1$.

Figures 3 and 4 illustrate the effect of microstructure characteristics of the b-fraction of a suspension on the behavior of the total scattering phase function. Dependences of $x(\theta)$ shown in Fig. 3 are obtained at different values of the modal radius, $r_m = 8$, 10, and 12 μm. The other parameters remained constant:

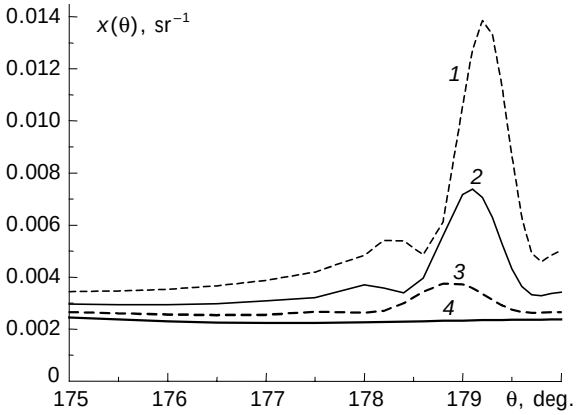

Fig. 3. The effect of modal radius $r_m = 12$ (*1*), 10 (*2*), and 8 μm (*3*) of particles of b-fraction on the dependences of $x(\theta)$ at $\nu = 2$, $p = 0.5$; the dependence of $px_t(\theta)$ (curve *4*).

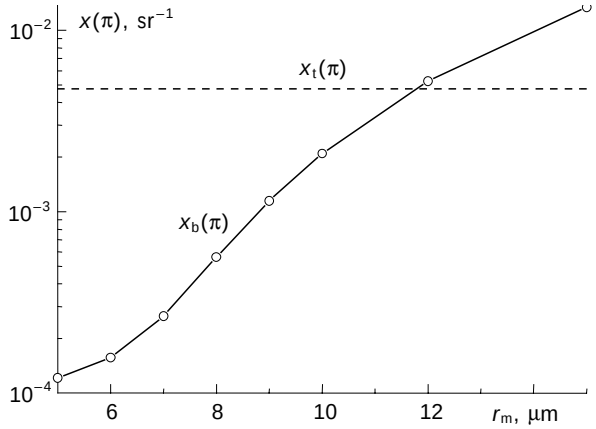

Fig. 4. The backscattering phase function $x_b(\pi)$ of the b-fraction as a function of the modal radius r_m (solid line); the level of the backscattering phase function $x_t(\pi)$ of the t-fraction at $\nu = 2$ (dashed curve).

$\nu = 2$ and $p = 0.5$. In spite of a marked increase of the role of t-fraction as compared with data in Fig. 1, on the given curves the noticeable diffraction peaks remain, as discussed previously. With the increase of the modal radius r_m the positions of the peaks of the curves are shifted closer to the scattering angle of 180°. The estimations of an effective particle size r_{eff} according to the peak position based on Eq. (8) are given in Table 1.

Table 1. Results of numerical simulation depending on the parameter r_m; $\nu = 2$; $p = 0.5$; $x_t(\pi) = 4.75_{10}-3$ sr^{-1}

r_m, μm	r_{eff}, μm	$x(\theta_1) / x(\pi)$	$x_b(\pi)$	$\xi_x(\pi)$	$\omega(\pi)$	$1 - \omega(\pi)$
8	9.43	1.41	$5.6_{10}-4$	8.5	0.89	0.11
10	12.6	2.16	$2.1_{10}-3$	2.27	0.69	0.31
12	14.1	2.77	$5.2_{10}-3$	0.9	0.48	0.52

The increase in r_m results also in the growth of the amplitude of the diffraction peaks. Table 1 shows the relations of the scattering phase function at the maximum of $x(\theta_1)$ to the value for the angle of 180° (the third column). From Fig. 3 and data given in Table 1 (the last column), it also follows that with the increasing modal radius r_m of b-fraction particles, their importance in the backscattering increases by several times.

These data are supplemented by Fig. 4, which shows the variation of the value $x_b(\pi)$ depending on the modal radius r_m. For a comparison Fig. 4 shows the level of the backscattering phase function $x_t(\pi)$ calculated at $\nu = 2$.

The amplitude of the diffraction peak near backward direction depends not only on the particle size. Figure 5 shows the effect of the refractive index of particles of the biogenic fraction on the behavior of the scattering phase functions. The results shown in Fig. 5, are obtained for the following values of the model parameters: $\nu = 2$; $r_m = 10$ μm; $p = 0.5$. The real part of the refractive index varied within the range $1.03 \le n_b \le 1.05$.

The pattern, shown in Fig. 5, in many cases is similar to the results shown in Fig. 3, except when the positions of curve maxima in Fig. 5 are not displaced relative to each other. When the index n_b tends to 1.03, the component $x_b(\theta)$ significantly decreases in the entire angular range considered, and the t-fraction of the suspended particles dominates in the total scattering phase function $x(\theta)$. With a decrease in n_b the diffraction peak becomes less pronounced.

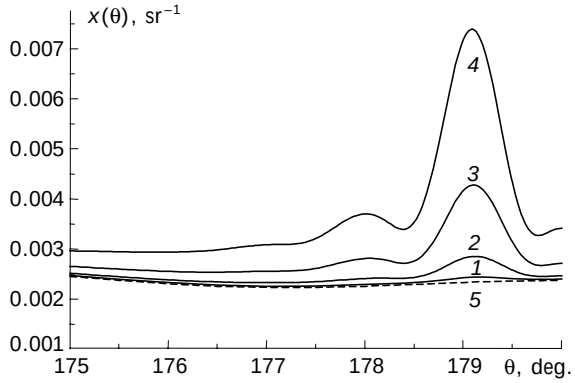

Fig. 5. The effect of the refractive index of particles of b-fraction $n_b = 1.035$ (*1*); 1.040 (*2*); 1.045 (*3*); 1.050 (*4*) on the scattering phase function $x(\theta)$ at $r_m = 10$ μm, $p = 0.5$; the dependence $px_t(\theta)$ (curve *5*).

The effect of microstructure of the t-fraction of suspended particles on the scattering phase functions is illustrated with the data depicted in Fig. 6 and presented in Table 2.

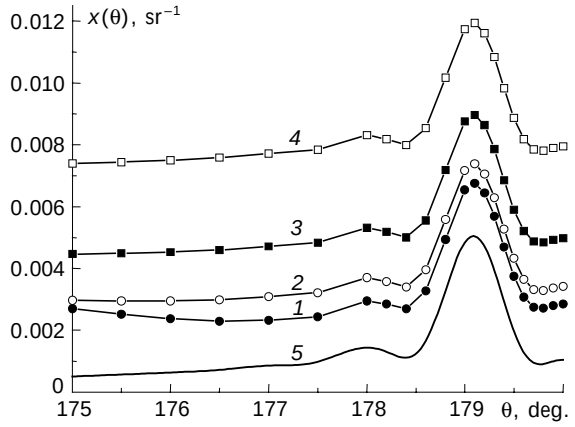

Fig. 6. The effect of disperse composition of t-fraction on the scattering phase function $x(\theta)$ at $\nu = 1$ (*1*); 2 (*2*); 2.5 (*3*); 3 (*4*) and $r_m = 10$ μm, $p = 0.5$; the dependence $(1 - p)x_b(\theta)$ at $\nu = 2$ (curve *5*).

The parameter ν varied in the range from 1 to 3. The other parameters had the following values: $r_m = 10$ μm; $p = 0.5$. The b-fraction of organic origin retained low microphysical composition, and its contribution to the total scattering phase function is shown by curve *5* in Fig. 6, with a typical diffraction peak near the scattering angle of 179.1°.

Table 2. Results of numerical simulation depending on the parameter ν; r_m = 10 μm, p = 0.5; $x_b(\pi) = 2.1_{10}-3$ sr^{-1}

ν	$x_t(\pi)$, sr^{-1}	$\xi_x(\pi)$
1	$3.63_{10}-3$	1.72
2	$4.75_{10}-3$	2.27
2.5	$7.88_{10}-3$	3.75
3	$1.38_{10}-2$	6.57

The role of particles of t-fraction is manifested in a systematic shift of the scattering phase function along the axis of ordinates. With the increasing value of ν, the role of the finest particles inside t-fraction becomes more important. This results in the increase of values of $x_t(\theta)$ in the considered angular range, and, as a result, in growth of the ratio $\xi(\theta)$. In particular, when changing ν from 1 to 3 the value $\xi(\pi)$ increases from 0.63 to 0.87.

Comparing the obtained results with a physical model of light scattering by seawater proposed by O.V. Kopelevich[1] it should be noted that, first, the backscattering phase function for t-fraction based on data from Ref. 1, $x_t(\pi) = 6.04_{10}-3$ sr^{-1}, is included between the appropriate values given in the second column of Table 2 for the parameter values ν = 2 and ν = 2.5.

Results of calculations for b-fraction, depicted in Fig. 4, show that close to a model level (Ref. 1), $x_b(\pi) = 2.24_{10}-4$ sr^{-1} the values of the backscattering phase function are obtained in the case when the modal particle radius r_m is within the range of 6 to 7 μm. With the increase of the modal radius when its value is ~ 12 μm the value of $x_b(\pi)$ is of the same order as $x_t(\pi)$. With the further increase of r_m b-fraction can be predominant in the backscattering.

The above-mentioned results make it possible to conclude:

1. The scattering phase function of t-fraction of the suspension in the angular range from 175 to 180° is a quasi-isotropic, and the level of the isotropic part depends on the contribution of the fine dispersion of the particle ensemble.

2. At the angular dependences of scattering phase functions of b-fraction of the suspension the diffraction peak (glory) at θ > 179° is observed, the position and amplitude of which strongly depend on the size and the refractive index of particles.

3. The ratio between the backscattering (θ = 180°) phase functions of t- and b-fractions is of one order of magnitude and higher, that determines, as a rule, the dominating contribution of t-fraction to the total scattering phase function $x(\theta)$.

4. The main contribution to the scattering phase function in the glory region, as a rule, depends on particles of b-fraction; the shape of the diffraction peak in the glory region does not depend on the level of the relative content of t-fraction.

Acknowledgments

The author would like to express his gratitude to G.P. Kokhanenko for constant attention to the work and useful discussion of results.

References

1. A.S. Monin, ed., *Ocean Optics,* Vol. 1. *Physical Ocean Optics* (Nauka, Moscow, 1983), 372 pp.
2. V.V. Veretennikov, Atmos. Oceanic Opt. **14**, No. 2, 146–152 (2001).
3. L.S. Dolin and V.A. Savel'ev, Izv. Akad. Nauk SSSR, Fiz. Atmos. Okeana **7**, No. 5, 505–510 (1971).
4. L.R. Bissonnette, Appl. Opt. **35**, No. 33, 6449–6466 (1996).
5. E.P. Zege, I.L. Katsev, and I.N. Polonskii, Izv. Ros. Akad. Nauk, Fiz. Atmos. Okeana **34**, No. 1, 45–50 (1998).
6. K.S. Shifrin, *Light Scattering in Turbid Water* (ONTI, Moscow–Leningrad, 1951), 288 pp.
7. H.C. van de Hulst, *Light Scattering by Small Particles* (Wiley, New York, 1957).